

Spectra of magnetoplasma excitations in back-gate Hall bar structures

V. M. Muravev,^{1,2} C. Jiang,¹ I. V. Kukushkin,^{1,2} J. H. Smet,¹ V. Umansky,³ and K. von Klitzing¹¹Max-Planck-Institut für Festkörperforschung, Heisenbergstrasse 1, 70569 Stuttgart, Germany²Institute of Solid State Physics, RAS, Chernogolovka 142432, Russia³Braun Center for Submicron Research, Weizmann Institute of Science, Rehovot 76100, Israel

(Received 6 December 2006; published 14 May 2007)

The microwave response of a two-dimensional electron system with a nearby *in situ* grown back gate has been investigated in transport. Several resonant absorption peaks are detected in the magnetoresistance and can be assigned to the excitation of collective magnetoplasma modes. The results are compared with data measured on a similar electron system but without gate. The two-dimensional plasma spectrum is drastically altered by the gate and exhibits a linear dispersion instead of the conventional square-root dependence anticipated from theoretical considerations.

DOI: 10.1103/PhysRevB.75.193307

PACS number(s): 71.35.Cc, 71.30.+h

There has been an increasing interest in the basic properties of robust collective phenomena such as plasma excitations in low-dimensional electron systems. An important impetus comes from potential applications of plasmons in the field of millimeter and submillimeter radiation detection. The main thrust is on two-dimensional plasmons in device structures based on single and double quantum wells^{1,2} or conventional field-effect transistors.^{3–5} The spectrum of plasmons in the two-dimensional electron system (2DES) in the long-wavelength limit ($k_F \gg q \gg \omega/c$) was calculated as early as 1967 by Stern⁶ as follows:

$$\omega_p^2(q) = \frac{n_s e^2}{2m^* \epsilon_0 \epsilon(q)} q. \quad (1)$$

Here, q is the wave vector of the plasmon, while n_s and m^* are the density and the effective mass of the two-dimensional (2D) electrons, respectively. The permittivity of vacuum and the effective permittivity of the surrounding medium are denoted as ϵ_0 and $\epsilon(q)$, respectively. This spectrum was experimentally verified in silicon inversion layers as well as for electrons on the surface of liquid helium.^{7–10}

The 2D plasmon spectrum possesses two features of particular relevance here: (i) it is gapless, i.e., the 2D plasmon frequency approaches zero as q approaches zero, and (ii) the plasmon frequency is perturbed by the geometry and dielectric properties of matter in the immediate vicinity of the 2D-electron system via the effective permittivity $\epsilon(q)$ in Eq. (1). For instance, if a gate is added underneath the 2D-electron layer, the 2D plasmon spectrum is described by the following expression:¹¹

$$\omega_p^2 = \frac{n_s e^2}{m^* \epsilon_0} \frac{q}{1 + \epsilon \coth qd}. \quad (2)$$

Here, d is the distance between the 2DES and the conducting gate layer. The above formula applies provided the distance of the 2DES from the top crystal surface d_1 fulfills the condition $qd_1 \ll 1$. From Eq. (2), we conclude that the 2D plasmon dispersion may be substantially modified merely by changing the parameter qd . In the limit $qd \gg 1$, the frequency follows the conventional square-root dependence on q . When

$qd \ll 1$ instead, the plasmon spectrum adopts the linear dependence described by

$$\omega_{AP}^2 = \frac{n_s e^2 d}{m^* \epsilon \epsilon_0} q^2. \quad (3)$$

We will refer to these excitations as acoustical plasmons. Previous studies of the dispersion of plasma excitations in gated systems were performed either in silicon based field-effect transistors (Refs. 7–9) or with 2D electrons on the surface of liquid helium (Ref. 10). For Si metal-oxide-semiconductor field-effect transistor, the plasmon spectrum was investigated with far-infrared transmission spectroscopy for the frequency range from 300 to 1000 GHz. In these experiments, coupling of the incident radiation to the plasmons was accomplished with the help of a grating, whose period defined the momentum of the plasma excitation. For electrons on a helium surface, the plasmon spectrum was determined by resonantly exciting standing plasma waves in the radio frequency range from 0.02 to 0.4 GHz. The momentum of the excitation in these measurements was set by the size of the 2D-electron system. To the best of our knowledge, in all these experiments, the value of qd always exceeded 0.25 ($qd=0.25$ in Ref. 7, $qd=0.27$ in Ref. 8, $qd=0.28$ in Ref. 9, and $qd=0.5$ in Ref. 10), and hence either the square-root dependence or the full, more complex functional dependence of Eq. (2) was valid. In this work, we address the unexplored regime with $qd \ll 1$ by investigating back-gated devices with mesas on the millimeter scale such that $qd \approx 0.02$. As many as three magnetoplasma modes with wave vectors determined by the transverse size of the structure were observed. They exhibited a linear dispersion consistent with the theoretical prediction of Eq. (3). The plasma velocity was investigated as a function of the electron density. A comparison of the linewidth of the resonances in a sample with and without back gate suggests that plasma damping is still mainly caused by electron relaxation processes and unaffected by the presence of a conducting back-gate layer.

The magnetoplasma excitations were detected by comparing the magnetoresistance R_{xx} traces acquired on a Hall bar geometry in the presence and absence of microwave radiation.^{12,13} When the microwave radiation is in resonance

with the plasmon frequency, the electron system is heated.¹⁴ The increase in the electron temperature is reflected in the sample resistivity, since scattering mechanisms are temperature dependent. Such experiments are most commonly performed by sweeping the magnetic field at a fixed frequency f_{res} of the incident radiation. The perpendicular magnetic field modifies the plasma spectrum. The plasma and cyclotron excitations hybridize, and the frequency of the combined mode is given by the formula¹⁵

$$\omega_{\text{hybrid}}^2 = \omega_{\text{AP}}^2 + \omega_c^2, \quad (4)$$

where $\omega_c = eB/m^*$ is the cyclotron frequency and ω_{AP} follows from Eq. (3). The magnetic-field dependence of ω_c ensures that a resonance will occur at some field provided the frequency of the incident radiation exceeds $\omega_{\text{AP}}/2\pi$. Since the cyclotron frequency is well known, the plasmon contribution ω_{AP} to the resonance frequency $\omega_{\text{hybrid}} = 2\pi f_{\text{res}}$ can easily be extracted.

The experiments were performed on a two-dimensional electron system located 135 nm below the top surface in an 18-nm-wide GaAs/AlGaAs quantum well. A 600-nm-thick n^+ -GaAs back gate (doping concentration of $2.3 \times 10^{18} \text{ cm}^{-3}$) was grown *in situ* at a distance d of 765 nm below the quantum well. Hall bars were patterned with a width of $W=0.1$ mm. The distance between adjacent voltage probes was equal to 0.5 mm. With the help of the back gate, the electron density n_s and electron mobility μ were tuned from 1.3×10^{11} to $2.8 \times 10^{11} \text{ cm}^{-2}$ and from 1.8×10^6 to $5.1 \times 10^6 \text{ cm}^2/\text{V s}$, respectively. A set of backward wave oscillators was used to generate radiation covering the frequency range of 13–80 GHz. The microwaves were guided to the sample via an oversized waveguide with a cross section of $19.0 \times 9.5 \text{ mm}^2$ (WG17). The waveguide was mounted in a cryostat with a superconducting coil and submerged in liquid helium. The sample was placed near the end of the waveguide in the Faraday geometry. The magnetoresistance was recorded with a standard lock-in technique by driving a sinusoidal current through the sample with a frequency of 13 Hz and an amplitude between 100–1000 nA. These experiments were carried out at a temperature of 1.6 K.

In Fig. 1, ρ_{xx} is plotted for a few different radiation frequencies. Also shown is ρ_{xx} if no microwave radiation is incident on the sample. At 25 GHz, a well-defined resonance develops near $B=51$ mT for both orientations of the magnetic-field. This resonance shifts to higher magnetic field values as the microwave frequency f increases and a second peak emerges at frequencies above 35 GHz. For instance, at $f=39$ GHz, two resonances appear and they are located at 90 and 44 mT. At even higher microwave frequencies, three resonances appear. An example at 66 GHz has been included. We will argue below that the observed resonances correspond to the excitation of different transverse (for $B=0$) magnetoplasma modes.

The origin of these resonances is best identified by plotting their magnetic-field positions versus the incident microwave frequency as in Fig. 2. The data were obtained at an electron density of $1.61 \times 10^{11} \text{ cm}^{-2}$. The data points coalesce onto three lines. In the strong magnetic-field limit, each

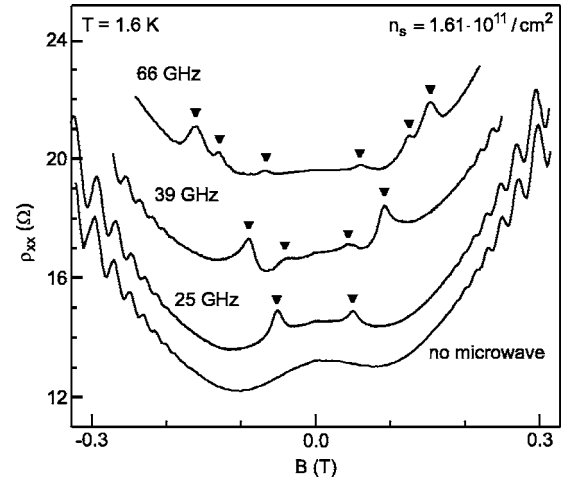


FIG. 1. The magnetoresistivity ρ_{xx} in the presence of 25, 39, and 66 GHz microwave radiation. For the sake of comparison, the ρ_{xx} trace in the absence of microwave radiation is also shown (bottom). Curves are offset for clarity. The microwave power inserted into the waveguide is approximately equal to 1 mW.

of these modes asymptotically merges into the cyclotron frequency line for an electron effective mass of $0.067m_0$. When fitting the magnetic-field dependence described by Eq. (4) to the data, the modes extrapolate to the following zero-field plasma frequencies: $f_1(0)=12.0$ GHz, $f_2(0)=35.3$ GHz, and $f_3(0)=60.1$ GHz. We assign each mode a wave vector $q = \pi N/W$. Since according to the dipole approximation^{16,17} a uniform microwave field can only excite modes with odd numbers, we only consider odd values of $N=1,3,5$. The linear dispersion of these plasma modes then becomes apparent in the inset in Fig. 2. For the sake of comparison, the dispersion of the 2D plasma modes observed in a Hall bar structure without an *in situ* grown back gate is shown in the same plot for the identical electron density. This Hall bar has

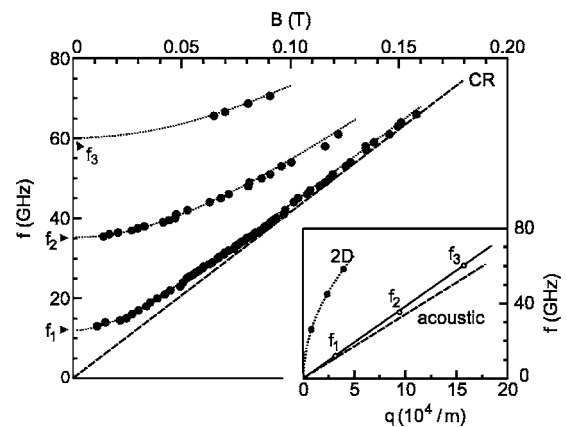


FIG. 2. The magnetic-field position of the absorption resonances versus excitation frequency. The microwave power inserted into the waveguide is approximately equal to 1 mW. The electron density is $1.61 \times 10^{11} \text{ cm}^{-2}$. The dotted line marks the magnetic-field dependence of the resonance position on frequency as predicted by Eq. (4). The inset shows the dispersion for the plasma waves in the 0.1-mm-wide sample with back gate (solid line) and in a reference structure without back gate with a width of 0.4 mm (dotted line).

a width of 0.4 mm instead of 0.1 mm. The plasmon dispersion in the back-gated sample indeed deviates considerably from the conventional square-root dependence seen in this ungated sample. We conclude that the observed modes are transverse (strictly transverse only for $B=0$) plasmon oscillations and the presence of the back gate has altered drastically the nature of these excitations. The influence of the nearby conducting back-gate layer may qualitatively be understood as follows. For the plasma wave propagating in the 2DES, the conducting back-gate layer partly screens the electric fields produced by the charge fluctuations associated with the plasma wave. The effect of screening is equivalent to placing an image charge equal in size but opposite in sign at a distance twice the spacer thickness separating back gate and 2DES, $2d$. The resulting fictitious out-of-phase bilayer charge wave possesses a linear dispersion in the small wave-vector region, $qd \ll 1$,¹⁸ and hence resembles an acoustical plasmon. Substituting in Eq. (3) the parameters $n_s = 1.61 \times 10^{11} \text{ cm}^{-2}$, $m^* = 0.067m_0$, $d = 765 \text{ nm}$, and $\epsilon = 12.8$ of our experiment, we obtain the predicted linear dispersion drawn as a dashed line in the inset in Fig. 2. It follows closely the experimental data. The calculation was performed assuming the following dielectric function $\epsilon(q)$:

$$\epsilon(q) = \frac{1}{2} \left(\frac{\epsilon \tanh qd_1 + 1}{\epsilon + \tanh qd_1} + \epsilon \coth qd \right).$$

It has been derived for a structure comprised of a 2DES in between a top and bottom layer with thicknesses d_1 and d , respectively, and with a conducting plane underneath.²⁰ This expression yields in the limit $qd_1 \ll 1$ the frequently used approximation for ω_p , Eq. (2). The deviation between experiment and theory can likely be ascribed to the inaccurate description of the dielectric environment surrounding the 2DES and/or the nonideal screening properties of the doped n^+ -GaAs back gate.

The presence of a back gate enables to tune the density over a wide range $(1.3\text{--}2.8) \times 10^{11} \text{ cm}^{-2}$. The bottom panel in Fig. 3 demonstrates that for a fixed microwave frequency, resonances move to higher values of the magnetic field when the electron concentration decreases. For each concentration, extrapolation based on Eq. (4) of data obtained at a set of frequencies (like in Fig. 2) is used to obtain the zero-field plasmon frequency of the fundamental mode $f_1(0)$. With the knowledge of $f_1(0)$, the velocity of the plasma excitations can be derived from $v_{AP} = 2\pi f_1(0)/q_1$, where $q_1 = \pi/W$ is the wave vector of the fundamental mode. The dependence of the plasma velocity v_{AP} on carrier concentration is depicted in the top panel of Fig. 3. The dotted line displays for comparison the theoretical estimate according to Eq. (3), which describes a square-root dependence.

Also shown in Fig. 3 is the Fermi velocity v_F . Even though adding a back gate to the system decelerates the plasmons, their velocity v_{AP} still fulfills the condition $v_{AP} \gg v_F$ for this heterostructure with $d = 0.765 \mu\text{m}$. Hence, Landau damping,¹⁹ i.e., collisionless plasma damping, only weakly contributes to the attenuation of the acoustical plasma excitations. Landau damping would only become significant when the distance between the 2DES and the back gate d is

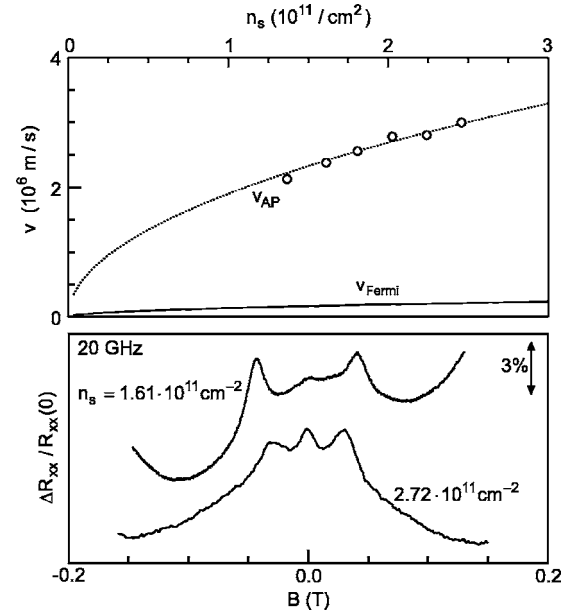


FIG. 3. Bottom panel: The magnetoconductance for 20 GHz incident radiation measured at two different electron densities n_s . The microwave power inserted into the waveguide is approximately equal to 1 mW. We note that the maximum at zero field does not depend on the frequency of the incident radiation. It is present even in the absence of radiation and hence specific to the magnetotransport properties of this heterostructure. Top panel: A comparison of the extracted plasma velocity for the sample with a back gate and the Fermi velocity as a function of the density. The dotted line is the theoretical estimate from Eq. (3).

smaller than 10 nm. In Fig. 4, the magnetoconductance for a sample with back gate and an ungated 2DES are compared at the same electron density to investigate differences in the resonance linewidths. The linewidth of the resonance Δf can easily be deduced from its width ΔB on the magnetic-field

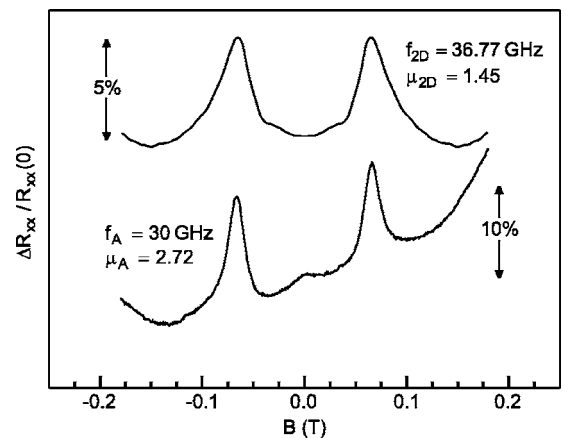


FIG. 4. The magnetoconductance R_{xx} under microwave radiation for the sample with back gate and 0.1 mm Hall bar width and an ungated Hall bar with a width of 0.4 mm measured at an electron density of $1.61 \times 10^{11} \text{ cm}^{-2}$. The upper curve is for the ungated sample, while the bottom one is for the sample with back gate. The frequency of the incident radiation and the mobility (in units of $10^6 \text{ cm}^2/\text{Vs}$) are included in the graph for both samples.

axis in Fig. 4 and the tangent of the magnetodispersion (as shown in Fig. 2 for the sample with gate) at the field where the resonance occurs, $\partial f/\partial B$, using the relation $\Delta f = (\partial f/\partial B)\Delta B$. At frequencies above 30 GHz, the plasmon excitations already approach the cyclotron line for both samples. Hence, at a given frequency, the ratio of the magnetic-field widths $\Delta B_{\text{ungated}}/\Delta B_{\text{backgated}}$ approximately equals the ratio of the frequency linewidths $\Delta f_{\text{ungated}}/\Delta f_{\text{backgated}}$. From Fig. 4, these ratios are estimated to be 2.1. This value approximately coincides with the ratio of the electron-scattering times $\tau_{\text{ungated}}/\tau_{\text{backgated}}$ determined from the zero-field mobility (1.9). This confirms that only

single-particle scattering contributes to the lifetime of the plasma excitations.

In conclusion, we have investigated the resonant absorption of microwave radiation using transport measurements on Hall bar samples containing a two-dimensional electron system with a buried back gate. Several plasma modes were detected. They exhibited a linear dispersion rather than the conventional square-root dependence on wave vector observed in ungated samples.

We acknowledge financial support from the RFFI, INTAS, DFG, the BMBF, the GIF, and the EU transnational access program (RITA-CT-2003-506095, WISSMC).

-
- ¹I. V. Kukushkin, S. A. Mikhailov, J. H. Smet, and K. von Klitzing, *Appl. Phys. Lett.* **86**, 044101 (2005).
²X. G. Peralta, S. J. Allen, M. C. Wanke, N. E. Harff, J. A. Simmons, M. P. Lilly, J. L. Reno, P. J. Burke, and J. P. Eisenstein, *Appl. Phys. Lett.* **81**, 1627 (2002).
³M. Dyakonov and M. Shur, *Phys. Rev. Lett.* **71**, 2465 (1993).
⁴F. Teppe, W. Knap, D. Veksler, M. S. Shur, A. P. Dmitriev, V. Yu. Kachorovskii, and S. Romyantsev, *Appl. Phys. Lett.* **87**, 052107 (2005).
⁵D. Veksler, F. Teppe, A. P. Dmitriev, V. Yu. Kachorovskii, W. Knap, and M. S. Shur, *Phys. Rev. B* **73**, 125328 (2006).
⁶F. Stern, *Phys. Rev. Lett.* **18**, 546 (1967).
⁷S. J. Allen, D. C. Tsui, and R. A. Logan, *Phys. Rev. Lett.* **38**, 17 (1977).
⁸D. Heitmann, J. P. Kotthaus, and E. G. Mohr, *Solid State Commun.* **44**, 715 (1982).
⁹T. N. Theis, J. P. Kotthaus, and P. J. Stiles, *Solid State Commun.* **26**, 603 (1978).
¹⁰C. C. Grimes and G. Adams, *Phys. Rev. Lett.* **36**, 145 (1976).
¹¹A. V. Chaplik, *Zh. Eksp. Teor. Fiz.* **62**, 746 (1972) [*Sov. Phys. JETP* **35**, 395 (1972)].
¹²I. V. Kukushkin, V. M. Muravev, J. H. Smet, M. Hauser, W. Dietsche, and K. von Klitzing, *Phys. Rev. B* **73**, 113310 (2006).
¹³E. Vasiliadou, G. Müller, D. Heitmann, D. Weiss, K. von Klitzing, H. Nickel, W. Schlapp, and R. Lösch, *Phys. Rev. B* **48**, 17145 (1993).
¹⁴A. Gold and V. T. Dolgoplov, *Phys. Rev. B* **33**, 1076 (1986).
¹⁵K. W. Chiu and J. J. Quinn, *Phys. Rev. B* **9**, 4724 (1974).
¹⁶For instance, S. A. Mikhailov and N. A. Savostianova, *Phys. Rev. B* **71**, 035320 (2005).
¹⁷C. Dahl, F. Brinkop, A. Wixforth, J. P. Kotthaus, J. H. English, and M. Sundram, *Solid State Commun.* **80**, 673 (1991).
¹⁸R. Z. Vitlina and A. V. Chaplik, *Zh. Eksp. Teor. Fiz.* **81**, 1011 (1981) [*Sov. Phys. JETP* **54**, 536 (1981)].
¹⁹L. D. Landau, *J. Phys. (USSR)* **10**, 27 (1946).
²⁰V. A. Volkov and S. A. Mikhailov, *Zh. Eksp. Teor. Fiz.* **94**, 217 (1988) [*Sov. Phys. JETP* **67**, 1639 (1988)].